Pergamon

PII: S0277-5387(96)00513-X

Polyhedron Vol. 16, No. 12, pp. 2047–2053, 1997

0277-5387/97 $17.00+0.00

Influence of chromium(III) on the formation of calcium hydroxyapatite

M. Wakamura, K. Kandori and T. Ishikawa*

School of Chemistry, Osaka University of Education, 4-698-1 Asahigaoka, Kashiwara-shi, Osaka-fu 582, Japan

(Received 14 June 1996; accepted 21 October 1996)

Abstract—Colloidal $Ca_{10}(PO_4)_6(OH)_2$(HA) particles doped with Cr^{3+} ions in different mole ratios (Cr/(Ca + Cr) = X_{Cr}) by a coprecipitation method were characterized by ICP, XRD, N_2 adsorption, TEM, EPMA, TG, XPS and FTIR. Ca^{2+} ions of HA were substituted by Cr^{3+} ions in one to one at $X_{Cr} \leqslant 0.13$. The particle size increased with an increase in X_{Cr}. When doped at $X_{Cr} \geqslant 0.13$ irregular particles were formed besides long rectangular particles containing Cr^{3+} ions less than *ca* 0.03 in X_{Cr}. The compositions of these two kinds of particles showed that the long rectangular particles were HA and the irregular particles were hydrated calcium chromium phosphate hydroxide. The growth of HA crystals was strongly promoted by doping Cr^{3+} ions.

Keywords: calcium hydroxyapatite; chromium(III); crystal growth; particle morphology; EPMA; XPS.

Calcium hydroxyapatite $Ca_{10}(PO_4)_6(OH)_2$ (noted HA) has been extensively investigated with the intention to use this material as adsorbents, catalysts and bioceramics. Since the structure and nature of HA depend on its nonstoichiometry, controlling of the stoichiometry is anticipated to generate materials having interesting functions. However, the chemical composition of HA is very sensitive to various preparation conditions, so that it is rather hard to regulate its nonstoichiometry reproducibly. The replacement of Ca^{2+} ions in HA with trivalent ions is a method to control its nonstoichiometry. The ion-exchange reaction of HA with trivalent ions such as Fe^{3+}, Al^{3+} and La^{3+} ions has been investigated in relation to their dental application [1–3]. On the other hand, there are few studies of the substitution by a coprecipitation method that can offer more pronounced modification of the HA structure compared with the ion-exchange method. In the previous study [4], we found that Fe^{3+} ions can be doped into HA up to *ca* 0.11 in mole ratio Fe/(Ca + Fe) with a coprecipitation method and resulted in reduction of the crystallinity and increase in the specific surface area. However, to establish the influence of trivalent ions on the formation and structure of HA, other trivalent ions having different sizes should be doped.

*Author to whom correspondence should be addressed.

This study was conducted to elucidate the effect of Cr^{3+} ions on the formation and structure of HA. The radius of this ion (0.069 nm) is closer to that of Ca^{2+} ions (0.099 nm) than that of Fe^{3+} ion (0.064 nm) used in the previous study and the solubility of chromium phosphate formed by coprecipitation is much lower than that of ferric phosphate. Thus, the effect of Cr^{3+} ions could be presumed to differ from that of Fe^{3+} ions. It is known that Cr^{3+} and Fe^{3+} ions are normally present in the organism [5]. The HA particles formed in the presence of different amounts of Cr^{3+} ions were characterized. The noticeable influence of this ion on the crystal growth of HA was found and the detailed results are reported in this paper.

EXPERIMENTAL

Materials

The preparation of the samples was done by a wet method. 0.1 mol of $Ca(NO_3)_2 \cdot 4H_2O$ was dissolved in 1 dm^3 deionized and distilled water free from CO_2. 0.060 mol H_3PO_4 were added to the $Ca(NO_3)_2$ solution and pH of the solution was adjusted to 9 by a 15 mol dm^{-3} NH_4OH solution. The resulting suspension was aged in a capped Teflon vessel at 100°C for 6 h. After the aging the precipitates were filtered off, washed

with 5 dm^3 deionized and distilled water and finally dried in an air oven at 70°C. Cr^{3+} ions were doped by adding $Cr(NO_3)_3$ to the $Ca(NO_3)_2$ solutions at mole ratios Cr/(Ca + Cr) varying from 0 to 1 before adding the NH_4OH solution.

Characterization

X-ray powder diffraction (XRD) of the obtained materials was done on a Rigaku high-intensity diffractometer using a CuK_α radiation (0.15418 nm) at 50 kV and 200 mA. P, Ca and Cr contents were determined by a Perkin-Elmer induced coupled plasma spectrometer (ICP). The samples for ICP were dissolved in a dilute HNO_3 solution. Morphology of the particles was observed on a Hitachi transmission electron microscope (TEM). To assay a single particle, electron probe microanalysis (EPMA) was carried out with a spot diameter of 1 nm. Thermogravimetry (TG) curves were recorded on a Rigaku thermoanalyser in an air stream at a heating rate of 5°C/min. X-ray photoelectron spectroscopy (XPS) were carried out by a Shimadzu XPS spectrometer. The binding energy was calibrated against O$1s_{1/2}$ peak. Infrared spectra (IR) were taken using a Digilab FTIR spectrometer by KBr method. The specific surface areas were evaluated by the BET method from N_2 adsorption isotherms measured by an automatic volumetric apparatus. Before the adsorption the samples were outgassed at 300°C for 2 h.

RESULTS AND DISCUSSION

Composition of Cr-doped HA

The Cr/(Ca + Cr) ratios of the formed particles were noted as X_{Cr} below. In Fig. 1 the X_{Cr} values are plotted against the Cr/(Ca + Cr) ratios of the starting solutions. The X_{Cr} values are almost equal to the Cr/(Ca + Cr) ratios of the starting solutions. This indicates that all of the Cr^{3+} ions added to the starting solutions are included in the formed particles. Figure 2 shows Ca and P contents of the formed particles as a function of X_{Cr}. With increasing X_{Cr}, the Cr content increases as shown by the open squares and the Ca content decreases as shown by the solid squares. At $X_{Cr} \leqslant 0.23$ both the contents linearly vary with X_{Cr}. The substitution ratio of Ca^{2+} ions with Cr^{3+} ions, that is, the number of Cr^{3+} ions replacing one Ca^{2+} ion was estimated from the slopes of the lines for Ca and Cr contents at $X_{Cr} \leqslant 0.23$. The substitution ratio amounted 1.0, meaning that Ca^{2+} ions are replaced by Cr^{3+} ions in one to one in spite of the charge difference between these ions. Hence no cation vacancy forms, leading to the production of excess positive charges. These positive charges could be compensated by formation of another compound on the HA surface and/or separately as confirmed by TEM later. The (Ca + Cr)/P ratios of the materials with varied X_{Cr} are shown by the circle symbols in Fig. 2. The ratios increase from 1.66 to 3.25 with increasing X_{Cr} from 0 to 1, being more than 1.67 of the stoichiometric ratio except the material without doping. Since CO_3^{2-} ions were not detected by FTIR but OH^- ions were detected, such large mole ratios would be ascribed to formation of another compound like chromium phosphate hydroxide. As will be described in the TEM result, irregular shaped particles were observed besides HA particles at $X_{Cr} \geqslant 0.13$ and increased with increasing X_{Cr} though no additional XRD peak appeared. It seems most likely therefore that another compound besides HA is generated.

Change of the crystal structure of HA

Figure 3 compares the XRD patterns of the materials formed in the presence of different amounts of Cr^{3+} ions. At X_{Cr} of 0.50 and less the patterns of all the materials possess only diffraction peaks due to

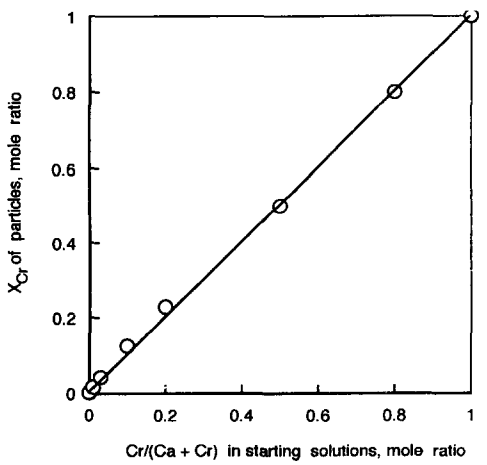

Fig. 1. Relationship between X_{Cr} of the formed particles and Cr/(Ca + Cr) in the starting solutions.

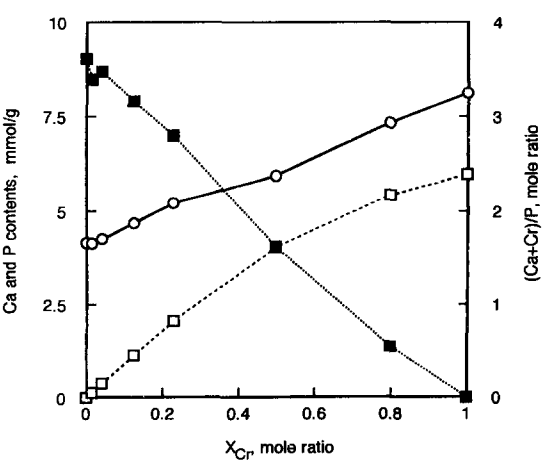

Fig. 2. Plots of Ca and Cr contents and (Ca + Cr)/P ratios against X_{Cr}; ■, Ca content; □, Cr content; ○, (Ca + Cr)/p.

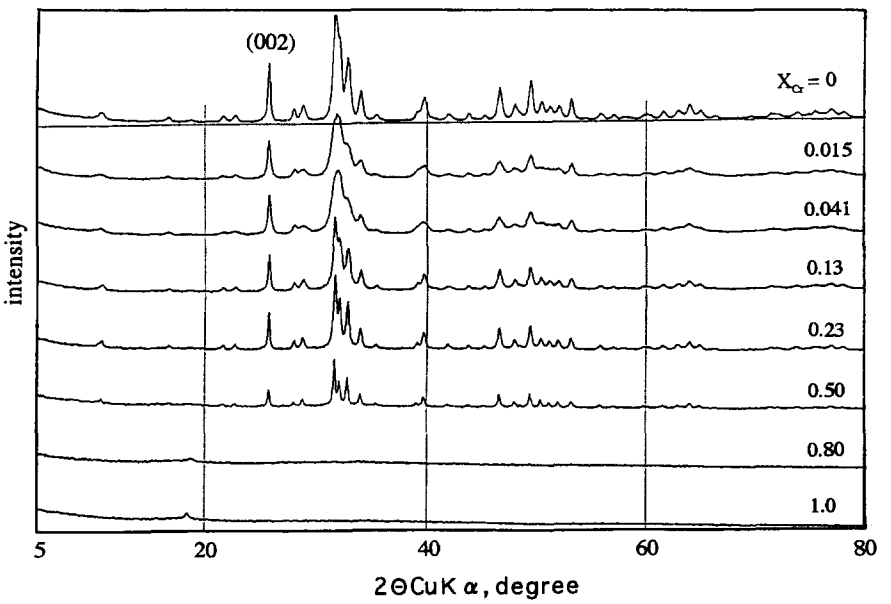

Fig. 3. XRD patterns of the materials with different X_{Cr}.

HA. The materials with $X_{Cr} = 0.015$ and 0.041 are less crystallized compared with other materials except for the materials with $X_{Cr} = 0.80$ and 1.00 showing only a weak peak at $2\theta = 17.3°$ that cannot be assigned for the moment. We estimated the influence of Cr^{3+} ions on the crystallinity of HA from half height width (noted HHW) of the XRD peak due to (002) plane. The HHW values are plotted against X_{Cr} by the open circles in Fig. 4. The materials with $X_{Cr} = 0.015$ and 0.041 show large HHW, which signifies that these materials have smaller crystallites and/or more distorted crystals. The change of crystallite sizes with doping can be estimated from the specific surface areas. The specific surface areas are shown along with the HHW values by the solid circles in Fig. 4. As seen in this figure the variation of surface area with X_{Cr} is well in accord with that of HHW. This reveals that the crystallite size is decreased by doping small amount of Cr^{3+} ions and increased with increasing X_{Cr} at $X_{Cr} \geqslant 0.13$. It is of interest that doping of Cr^{3+} ions results in the growth of HA crystallites.

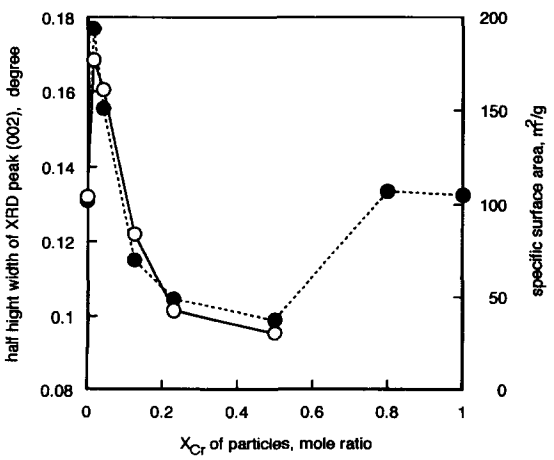

Fig. 4. Half height width (HHW) of XRD peak due to (002) plane (open symbols) and specific surface area (full symbols) of the materials with varied X_{Cr}.

Morphology of Cr-doped HA particles

Figure 5 displays TEM pictures of the materials doped with different amounts of Cr^{3+} ions. The HA particles without doping are small short needles and they grow into large long particles upon increasing X_{Cr}. However, the larger particles with $X_{Cr} \leqslant 0.13$ have higher surface area and larger HHW compared to the particles without doping and with $X_{Cr} \geqslant 0.13$ (Fig. 4). Thus, the particles with $X_{Cr} = 0.015$ and 0.041 seem to be agglomerates of minute primary particles as observed in the TEM pictures. The materials with $X_{Cr} = 0.13$, 0.23 and 0.50 are made up of long thin rectangular particles and a small amount of irregular particles. The irregular particles increase as X_{Cr} increases. At $X_{Cr} \geqslant 0.80$ no long rectangular particles are observed and only small cube-like particles are observed. The irregular and cube-like particles are supposed to be not HA. To verify this, we carried out EPMA on the materials with $X_{Cr} = 0.041$ and 0.13. Ca, Cr and P contents of thin long particles in the material with $X_{Cr} = 0.041$ and both thin long and irregular particles in the material with $X_{Cr} = 0.13$ were determined. Table 1 shows the contents averaged for 10 particles of each kind of particles. The mole ratios of X_{Cr} and (Ca + Cr)/P measured by EPMA on the particles with $X_{Cr} = 0.041$ are close to X_{Cr} and (Ca + Cr)/P obtained by ICP, respectively, taking account of the deviations. On the other hand, in the

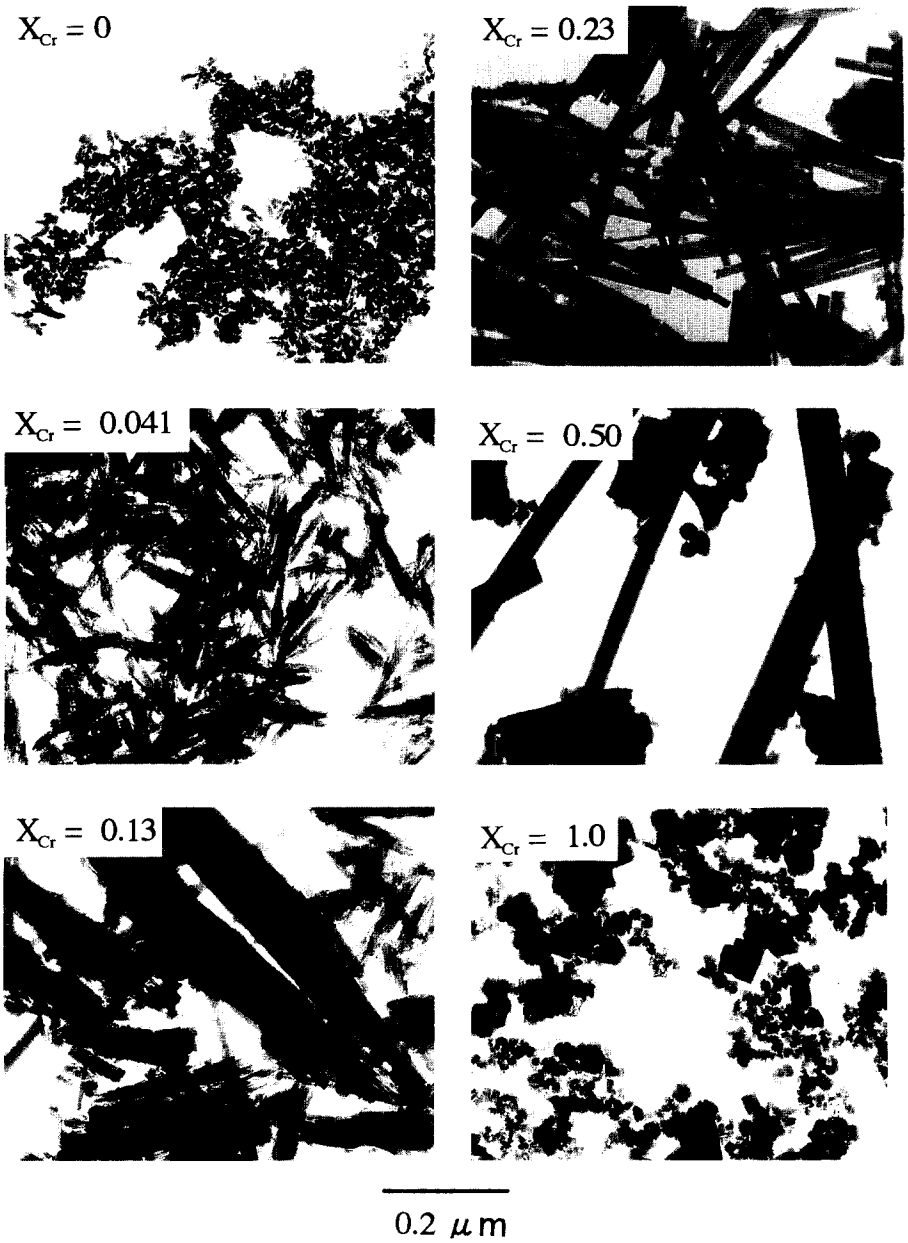

Fig. 5. TEM pictures of the materials with different X_{Cr}.

Table 1. X_{Cr} and (Ca + Cr)/P of the materials with X_{Cr} = 0.041 and 0.13 determined by ICP and EPMA

X_{Cr}		(Ca + Cr)/P	
ICP	EPMA	ICP	EPMA
0.041	0.046 ± 0.021	1.71	1.56 ± 0.31
	0.026 ± 0.008[a]		1.50 ± 0.30[a]
0.13		1.87	
	0.71 ± 0.08[b]		3.2 ± 0.1[b]

Symbols [a] and [b] represent long rectangular particles and irregular ones, respectively.

case of the material formed with $X_{Cr} = 0.13$, the irregular and long rectangular particles show quite different X_{Cr} and (Ca + Cr)/P determined by EPMA; the irregular particles show larger mole ratios than the long rectangular ones. It is clear from these EPMA results that the irregular particles are not HA and the long rectangular particles are HA. From the EPMA and IR results shown later, the composition formula of the irregular particles in the material with $X_{Cr} = 0.13$ is expressed as $Ca_{0.3}Cr_{0.7}(PO_4)_{0.3}(OH)_{1.8}$ using $X_{Cr} = 0.71$ and (Ca + Cr)/P = 3.2 shown in Table 1. This substance is hydrated as shown by TG and it is less crystalline since no XRD additional peak appeared (Fig. 3). As shown in Fig. 2, (Ca + Cr)/P ratio increased from 1.66 to 3.3 with increasing X_{Cr} from 0 to 1.0. This can be explained by the formation of another compound with a large (Ca + Cr)/P ratio. At $X_{Cr} \geqslant 0.13$, this compound forms as irregular particles, as shown by TEM. The composition formula of the cube-like particles formed without Ca^{2+} ions ($X_{Cr} = 1.0$), estimated from the Cr and P contents determined by ICP, is $Cr_{3.3}(PO_4)(OH)_{6.9}$. This material is also hydrated as will be shown.

Thermal analysis of Cr-doped HA

To examine the thermal stability of Cr-doped HA, TG curves of the materials with varied X_{Cr} were measured. The TG curves are shown in Fig. 6. The material without doping gives rise to continuous weight loss continued to 1000°C, which is mainly due to adsorbed and/or strongly bound H_2O as has been confirmed by FTIR [6]. The materials with $X_{Cr} \geqslant 0.13$ show a small weight loss from *ca* 550°C in addition to the weight loss observed on the material without doping. This weight loss may be due to the release of OH^- ions as H_2O in the irregular particles. The total weight loss markedly increases with increasing X_{Cr}, showing that the materials with larger X_{Cr} contain more OH^- ions as speculated from the composition proposed above. However, the weight loss due to dehydroxylation of the material with $X_{Cr} = 1.0$, estimated from the composition $Cr_{3.3}(PO_4)(OH)_{6.9}$, amounts to 16.2 wt.%, much smaller than the weight loss of 38.8 wt.% at 25 to 1000°C in the TG curve. This large weight loss seems to be attributable to release of the bound H_2O. Consequently, the composition of the material with $X_{Cr} = 1.0$ can be regarded as $Cr_{3.3}(PO_4)(OH)_{6.9} \cdot 7.9H_2O$.

XPS and IR spectra of Cr-doped HA

XPS spectra of the samples with different X_{Cr} were taken to clarify the state of Cr^{3+} ions doped in HA. Figure 7 shows the peaks due to $P2p_{2/3}$, $Ca2p_{1/2}$, $Ca2p_{3/2}$ and $Cr2p_{3/2}$ of the materials with different X_{Cr}. These peaks are not markedly shifted by doping. The binding energy of $Cr2p_{3/2}$ peak is 577.5 to 577.9 eV. The binding energies of $Cr2p_{3/2}$ peaks determined on various chromium compounds are 573.8(metal Cr), 576.7(Cr_2O_3), 578.8(CrF_3), 579.2(CrO_3) and 579.9 eV($K_2Cr_2O_7$). Since the binding energy of $Cr2p_{3/2}$ peak for Cr-doped HA lies between those for Cr_2O_3 and CrF_3, the doped Cr^{3+} ions seem to exist as trivalent ions. Furthermore, the binding energy of 577.9 eV of the material with $X_{Cr} = 0.041$ is close to 577.8 eV of the material with $X_{Cr} = 1.0$ of which the formula is $Cr_{3.3}(PO_4)(OH)_{6.9} \cdot 7.9H_2O$. It seems therefore that the

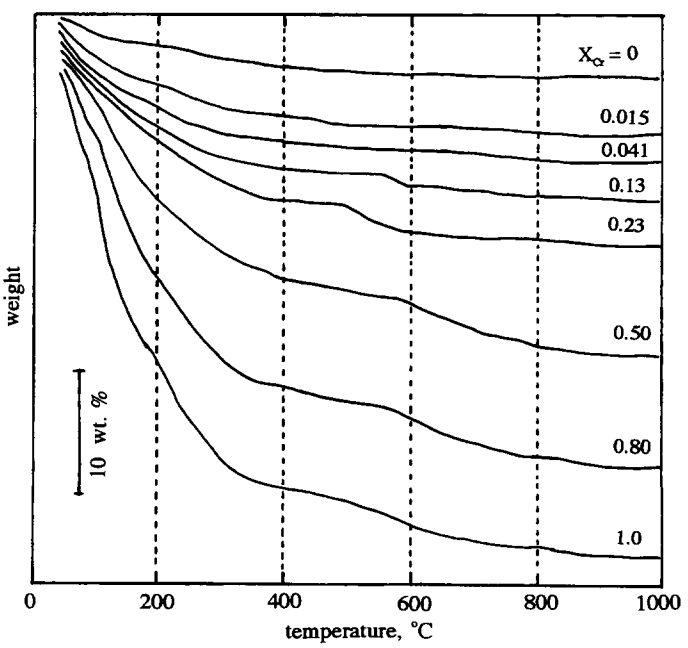

Fig. 6. TG curves of the materials with different X_{Cr}.

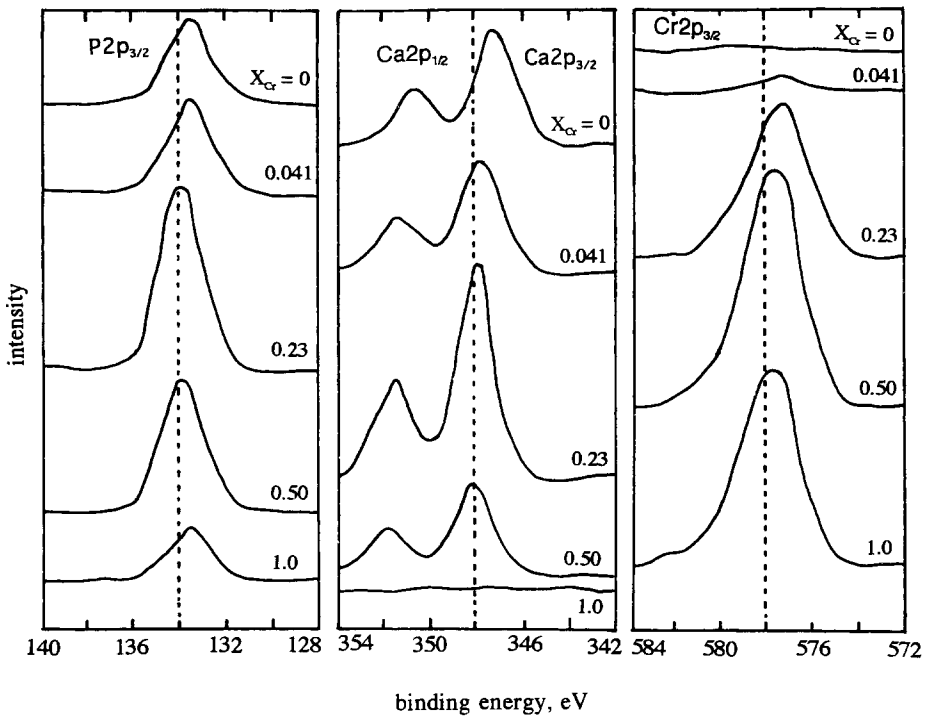

Fig. 7. XPS spectra of the materials with different X_{Cr}.

doped Cr^{3+} ions are coordinated by OH^- and PO_4^{3-} ions and H_2O molecules.

As mentioned already, less-crystallized irregular particles formed with larger X_{Cr} are supposed to be hydrated chromium phosphate hydroxide, for instance, such as $Cr_{3.3}(PO_4)(OH)_{6.9} \cdot 7.9H_2O$ for the material with $X_{Cr} = 1.0$. For further verification of this, IR spectra of the materials with varied X_{Cr} were measured and are depicted in Fig. 8. The spectrum of the material without doping shows the bands at 1090 and 1040 cm^{-1} due to the stretching mode (ν_3) of O—P, the weak bands at 960 cm^{-1} due to the stretching mode (ν_1) of O—P and the bands at 630, 605 and 560 cm^{-1} due to the deformation mode (ν_4) of O—P—O [7]. The intensities of these PO_4-bands increase with increasing X_{Cr} and the PO_4-bands of the material with $X_{Cr} = 0.13$ are very strong. At $X_{Cr} \geqslant 0.23$ the PO_4-bands are weakened with increasing X_{Cr} and are very broad at $X_{Cr} \geqslant 0.80$. These FTIR results are in good agreement with the XRD results; highly crystallized materials give rise to strong sharp PO_4-bands. The materials with $X_{Cr} \geqslant 0.80$ show a strong broad band centered at 3400 cm^{-1} with a shoulder at 3200 cm^{-1} due to the stretching modes of OH^- ions and stretching modes (ν_1 and ν_3) of H_2O molecules, and a strong band at 1630 cm^{-1} due to the deformation mode (ν_2) of H_2O molecules, although the spectra are not shown here. This proves that the material with $X_{Cr} \geqslant 0.80$ contains larger amount of OH^- ions and H_2O molecules compared to the other materials, supporting the proposed chemical composition.

Effect of Cr^{3+} ions on the crystal growth of HA

As seen from Fig. 5, doping of Cr^{3+} ions causes a marked growth of HA particles. Such uniform large particles observed in the materials with $X_{Cr} = 0.23$ and 0.50 shown in Fig. 5 did not form when substituted with Mg^{2+} ions by a precipitation method, while large agglomerates of small primary HA particles were produced [8]. It has been reported that the ion-exchange of HA with Fe^{3+}, Al^{3+} and La^{3+} ions in acidic solutions destroys the HA crystals to form phosphates of these ions [1–3]. However, the crystal growth of HA found in the present study did not take place in the ion-exchange. Various trivalent ions such as Al^{3+}, Cr^{3+} and La^{3+} ions reduce the dissolution of HA in solutions less than pH 7 but Fe^{3+} ions do not influence this [9–11]. This effect can be explained by the formation of phosphates of the former three ions with lower solubility than HA. However, the materials of this study were synthesized in basic solutions of pH 9 where the solubility of HA is much lower than that of metal phosphates [12]. Hence, the hydrated chromium phosphate hydroxide resulted by doping of Cr^{3+} ions would not influence dissolution of HA particles. According to the EPMA result, long rectangular HA particles formed with $X_{Cr} \leqslant 0.13$ contain Cr^{3+} ions less than *ca.* 0.03 in X_{Cr}. Such a small amount of Cr^{3+} ions cannot interfere with the crystal growth of HA. The Cr^{3+} ions doped at $X_{Cr} >$ *ca* 0.03 are consumed to produce hydrated calcium chromium phosphate hydroxide that is less-crystallized irregular particles. This substance is considered to control the crystal

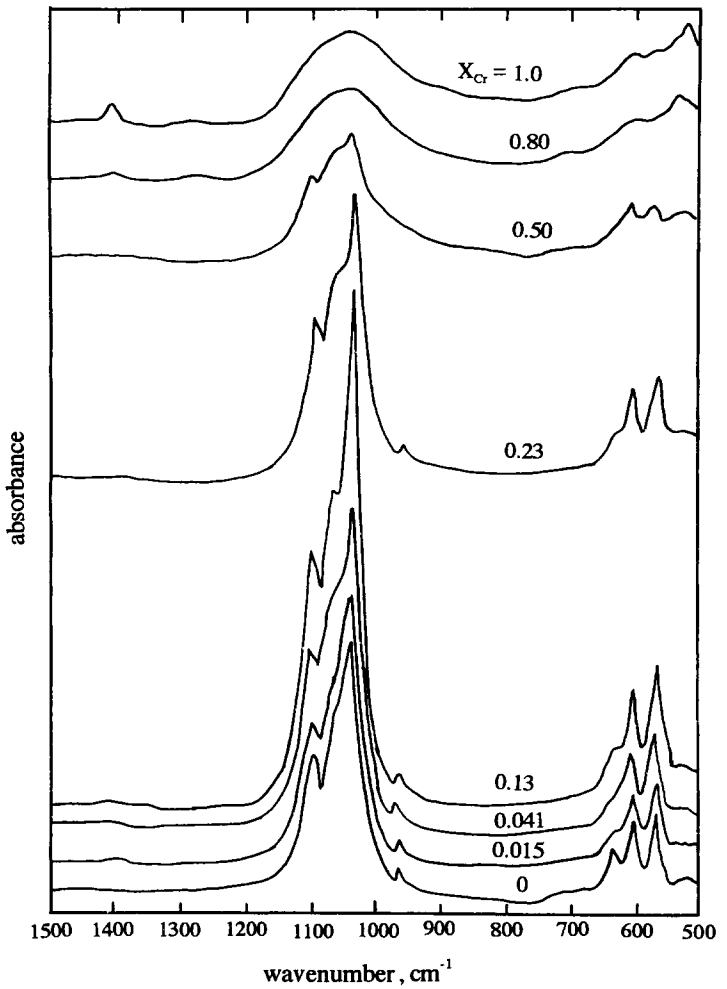

Fig. 8. IR spectra of the materials with different X_{Cr}.

growth of HA by decreasing the number of precursor nuclei and acting as the reservoir of the solutes for the crystal growth.

In conclusion, the crystal growth of HA is strongly promoted on doping Cr^{3+} ions by the coprecipitation method with basic solutions. Long rectangular HA particles resulted on doping at $X_{Cr} \geqslant 0.23$, containing a small amount of Cr^{3+} ions. The residual doped Cr^{3+} ions are consumed to produce hydrated calcium chromium phosphate hydroxides which concern the crystal growth of HA.

Acknowledgements—This study was supported in part by Nippon Sheet Glass foundation for Materials Science and Technology and the Grants-in-Aid for Scientific Research (B) and (C) of the Ministry of Education, Science, Sports and Culture, Japan.

REFERENCES

1. Y. Tanizawa, K. Sawamura and T. Suzuki, *J. Chem. Soc., Faraday Trans.* 1990, **86,** 1071.
2. Y. Tanizawa, K. Sawamura and T. Suzuki, *J. Chem. Soc., Faraday Trans.* 1990, **86,** 4025.
3. T. Suzuki and T. Hatsushika, *Gypsum Lime* 1990, **244,** 15.
4. T. Ishikawa, H. Saito, A. Yasukawa and K. Kandori, *Bull. Chem. Soc. Jpn.* 1996, **69,** 899.
5. J. A. Weatherell and C. Robinson, *Proc. Finn. Dent. Soc.* 1982, **78,** 81.
6. T. Ishikawa, M. Wakamura and S. Kondo, *Langmuir* 1989, **5,** 140.
7. J. C. Elliott, *Structure and Chemistry of the Apatites and Other Calcium Orthophosphates*, p. 171. Elsevier, Amsterdam (1994).
8. A. Yasukawa, S. Ouchi, K. Kandori and T. Ishikawa, *J. Mater. Chem.* 1996, **6,** 1401.
9. M. R. Christoffersen and J. Christoffersen, *Calcif. Tissue Int.* 1985, **37,** 673.
10. M. R. Christoffersen, H. C. Thyregod and J. Christoffersen, *Calcif. Tissue Int.* 1987, **41,** 27.
11. P. Schaad, P. Gramain, F. Gorce and J. C. Voegel, *J. Chem. Soc., Faraday Trans.* 1994, **90,** 3405.
12. W. Stumm and J. J. Morgan, *Aquatic Chemistry* p. 283. Wiley Interscience, New York (1981).